Journal of Materials Chemistry A

PAPER

View Article Online
View Journal | View Issue

Cite this: J. Mater. Chem. A, 2015, 3, 7799

Strongly acidic mesoporous aluminosilicates prepared *via* hydrothermal restructuring of a crystalline layered silicate†

Nurul Alam and Robert Mokaya*

Received 22nd January 2015
Accepted 3rd March 2015

DOI: 10.1039/c5ta00548e

www.rsc.org/MaterialsA

We describe the preparation of crystalline as-synthesized aluminosilicate–surfactant mesophases and surfactant-free aluminosilicate mesoporous materials derived from the layered silicate Na-RUB-18, by performing hydrothermal restructuring in the presence of cetyltrimethylammonium (CTA) surfactant molecules. The hydrothermal treatment, at 150 °C for 48 h, with Na-RUB-18 as the silica source and a known amount of aluminium isopropoxide (gel Si/Al ratio 5, 10 or 20) in the presence of cetyltrimethylammonium (CTA) ions generates molecularly ordered aluminosilicate–surfactant mesophases. The transformation from mesophases to mesoporous materials takes place with retention of mesostructures with varying levels of crystallinity depending on the mode of template removal. The highest apparent retention of crystallinity in a surfactant-free mesostructure is achieved at Si/Al ratio = 20 after surfactant removal *via* solvent extraction in acidified ethanol. The textural properties of the mesoporous materials (surface area in the range of 141–388 $m^2\ g^{-1}$ and pore volume in the range of 0.12–0.46 $cm^3\ g^{-1}$) depend on the mode of surfactant removal and Si/Al ratio. The mesoporous aluminosilicates are strongly acidic with most of the acid sites generated (>80% and typically above 95%) classified as strong sites and exhibit attractive activity as solid acid catalysts.

1. Introduction

Mesoporous molecular sieves of the M41S family are attractive for a variety of applications due to their well-ordered mesopores, high surface area and pore volume.[1–4] Over the past decade a variety of assembly pathways have been developed for the synthesis of hexagonal (MCM-41),[1–5] cubic (MCM-48),[6] wormhole (HMS, MSU-X),[7] lamellar-vesicular (MSU-G),[8] 2D hexagonal (SBA-15),[9] and foam-like (MFC, MSU-F)[10] mesoporous materials. Mesoporous aluminosilica materials have attracted much attention due to their potential use in various applications including in heterogeneous catalysis (especially as catalysts and catalyst supports for large molecular transformations), sorption, molecular sieving and hard-templating.[2–4,11] In general, despite excellent structural ordering, most mesoporous silica and aluminosilica possess pore walls that are amorphous, which means that they have poor stability, weak acidity, and low ion exchange capacity. This places limitations on their use as solid acids and ion exchangers. Efforts to address these limitations have resulted in the formation of composite zeolite/mesoporous materials *via* a number of pathways including (i) the assembly of preformed nanoclustered zeolite seeds,[12] (ii) partial recrystallization of the interporous surface of mesoporous aluminosilicates,[13] (iii) transformation[14] or coating[15] of the amorphous walls of mesoporous aluminosilicates into semicrystalline pseudo-zeolitic frameworks, (iv) the use of partially crystallized zeolite colloidal gels[16] or zeolites[17] as precursors, and (v) dual templating with both long chain surfactant molecules and small chain amines.[18] Stable mesoporous aluminosilicates with high acidity have also been prepared *via* post-synthesis grafting of heteroatoms onto mesoporous silica.[19–21] The synthesis of the so-called mesoporous zeolites has been more recently reported,[22] wherein the use of amphiphilic surfactant template molecules with three components (a hydrolysable methoxysilyl moiety, a quaternary ammonium moiety and a hydrophobic alkyl chain moiety) is a key factor in the formation of crystalline materials.

The formation of silica–surfactant mesophases that exhibit molecular ordering can be achieved *via* direct mixed-gel synthesis routes that utilize conventional alkylammonium surfactants as structure directing agents.[23] The formation of molecularly ordered domains in mesoporous silica and aluminosilica has also been achieved *via* extended crystallization at 150 °C.[24] However, in general, molecularly ordered silicate–surfactant mesophases are unstable to template removal.

School of Chemistry, University of Nottingham, University Park, NG7 2RD Nottingham, UK. E-mail: r.mokaya@nottingham.ac.uk; Fax: +44 (0) 115 951 3562; Tel: +44 (0) 115 846 6174

† Electronic supplementary information (ESI) available: Ten additional figures; the powder XRD pattern of parent Na-RUB-18, DTG profiles, IR spectra, TEM images, SAED patterns and SEM images of as-synthesised mesophases and surfactant-free materials, and powder XRD patterns and IR spectra of extracted or oxidised surfactant-free samples before and after calcination. See DOI: 10.1039/c5ta00548e

Indeed, template removal is a key factor in any attempts to transform molecularly ordered silicate–surfactant (alkylammonium) mesophases into template-free crystalline mesoporous materials; whereas template removal *via* calcination destroys the mesoporosity and molecular ordering,[24] recent work has shown that benign template removal may be used to generate surfactant-free mesostructured materials that retain molecular ordering. In this regard, layered zeolite-like precursors offer a well established route to amorphous mesoporous silica.[25] To retain crystallinity, it is necessary that mesophases derived from layered zeolitic precursors are formed *via* folding of layers or *via* fragmentation that retains molecular ordering.[24,26] Here we report on the preparation of aluminosilicate–surfactant mesophases and surfactant-free aluminosilicate mesoporous materials derived from the layered silicate Na-RUB-18. We probe the effect of mode of template removal on molecular ordering and textural properties and discuss the nature of incorporated Al and generated acidity.

2. Experimental

2.1 Synthesis of materials

2.1.1 Preparation of layered silicate Na-RUB-18. The layered silicate was prepared using established procedures.[27,28] Briefly, 0.94 g of NaOH was dissolved in 183.8 g of water at 50 °C, followed by addition of 15 g of hexamethylenetetramine ($C_6H_{12}N_4$) and 40 g of sodium trisilicate hydrate ($Na_2Si_3O_7 \cdot H_2O$). After 1 h of stirring, the gel was loaded into Teflon-lined autoclaves and heated statically at 100 °C for 1 month. The resulting Na-RUB-18 powder was recovered by filtration, washed with water and ethanol, and dried at room temperature.

2.1.2 Preparation of surfactant–aluminosilicate mesophases. Surfactant–aluminosilicate mesophases were prepared from aqueous suspensions of layered silicate Na-RUB-18, aluminium isopropoxide and cetyltrimethylammonium (CTA) ions. Briefly, 1.14 g of Na-RUB-18 powder was added to a solution containing a known amount of aluminum isopropoxide (to achieve a Si/Al ratio of 5, 10 or 20), 20 ml of 0.1 M CTACl and 3 ml of 0.1 M CTAOH. After refluxing at 80 °C for 3 h, the suspension was statically heated in Teflon-lined autoclaves at 150 °C for 48 h. The solid products were recovered by filtration, washed with water and ethanol, and dried at room temperature to yield the as-synthesized samples designated as surfactant–aluminosilicate mesophases.

2.1.3 Surfactant removal from aluminosilicate mesophases

(i) H_2O_2-mediated oxidation of the surfactant. In a typical process, 0.6 g of the as-synthesized aluminosilicate mesophase was dispersed under stirring in 5 ml of H_2O containing 12 mg of $FeCl_3 \cdot 6H_2O$. This was followed by the addition of 50 ml of 30% H_2O_2 drop-by-drop. After being stirred overnight at room-temperature, the sample was recovered by filtration. To ensure the complete removal of the surfactant, the H_2O_2-mediated oxidation procedure was repeated twice. The resulting samples are referred to as "oxidised".

(ii) Solvent extraction of the surfactant. In a typical extraction process, 0.5 g of the as-synthesized aluminosilicate mesophase was refluxed in 60 ml of 4 wt% HCl/ethanol solution at 60 °C for 3 h. The refluxing procedure was repeated twice to ensure the complete removal of the surfactant. The resulting samples are designated as "extracted".

(iii) Calcination. (a) The as-synthesized aluminosilicate mesophases were calcined at 450 °C under a flow of nitrogen gas (100 ml min^{-1}) for 1 h and then in flowing air (100 ml min^{-1}) for 6 h. The thermally treated samples are designated as "calcined".

(b) Surfactant-free mesoporous aluminosilicates, previously extracted or oxidized, were calcined at 450 °C under a flow of nitrogen gas (100 ml min^{-1}) for 1 h and then in flowing air (100 ml min^{-1}) for 6 h. The thermally treated samples are designated as "EXT + CAL" and "OXI + CAL".

2.2 Characterization

Elemental composition (Si/Al ratio) was determined using a Philips MiniPal PW4025 X-ray fluorescence (XRF) instrument. Powder XRD analysis was performed using a Bruker AXS D8 Advance powder diffractometer with Cu Kα radiation (40 kV, 40 mA), 0.020° step size, and 1 s step time and a Philips 1830 powder diffractometer with Cu Kα radiation (40 kV, 40 mA), 0.020° step size, and 1 s step time. The textural properties were determined *via* nitrogen sorption analysis at −196 °C using a conventional volumetric technique on a Micromeritics ASAP 2020 sorptometer. Before analysis the samples were oven dried at 150 °C and evacuated overnight at 150 °C. The surface area was calculated using the BET method applied to adsorption data in the relative pressure (P/P_o) range of 0.05 to 0.2. The total pore volume was estimated on the basis of the amount of nitrogen adsorbed at a relative pressure of *ca.* 0.99. The pore size distribution was determined using the Barrett–Joyner–Halenda (BJH) method applied to adsorption data. Thermogravimetric analysis was performed using a Perkin Elmer Pyris 6 TG analyzer (heating rate of 5 °C min^{-1}) in static air or a TA Instruments SDT Q 600 analyzer (heating rate of 5 °C min^{-1}) in static air or flowing nitrogen conditions. A Bruker optics TENSOR 27 series FT-IR spectrometer was used to obtain IR spectra. ^{27}Al MAS NMR spectra were acquired at a frequency of 104 MHz, an acquisition time of 10 ms, a recycle delay of 0.1 s, a spectral width of 416 kHz and a MAS rate of 14.0 kHz. Transmission electron microscopy (TEM) images were recorded on a JEOL 2000-FX electron microscope operating at 200 kV. Scanning electron microscopy (SEM) images were recorded using a FEI XL30 microscope. Samples for analysis were prepared by spreading them on a holey carbon film supported on a grid.

To determine the acid content, the samples were exposed to liquid cyclohexylamine (CHA) at room temperature overnight and then heated in an oven at 80 °C for 2 h. TGA curves were then obtained for the CHA-containing samples and the mass loss associated with desorption of the base from acid sites was used to calculate the acid content as mmol of CHA per gram of samples assuming that each acid site (*i.e.*, H^+) interacts with one base molecule.[29,30] To obtain the content of strong acid sites, the CHA-containing samples already dried at 80 °C were further heated in an oven at 250 °C prior to TGA.

The acidity and catalytic activity of the calcined aluminosilicate materials were assessed for the dehydration of pentan-1-

o1, which was performed in pressure vessels at 200 °C for 4 h with 0.3 g of catalyst and 3.0 ml of reactant. The pressure vessels were placed in an oven at 200 °C for the duration of the reaction and then immersed in ice to quench the reaction. The reaction products were recovered and analysed using gas chromatography.

3. Results and discussion

3.1 Elemental composition and structural ordering

The XRD pattern of the Na-RUB-18 layered silicate material (ESI Fig. S1†) is consistent with XRD patterns reported in the literature;[28,31] the observed XRD peaks are characteristic of layered silicate RUB-18, which confirmed the crystallinity and purity of our starting material. The XRD pattern of the layered silicate is dominated by a sharp (004) peak at $2\theta = 7.7°$, corresponding to an inter-layer spacing of 11.1 Å. The purely siliceous Na-RUB-18 material was used as the 'silica source' in the presence of Al in the preparation of aluminosilicate materials. The elemental composition of the as-synthesised (AS) aluminosilicate mesophases is given as the Si/Al ratio in Table 1 and is in all three cases close to the synthesis gel composition. The powder XRD patterns of the as-synthesized aluminosilicate–surfactant mesophases, shown in Fig. 1, indicate the formation of an expanded layered material that coexists with a mesostructured phase. The presence of the expanded layered material is indicated in Fig. 1 by the shift of the (004) peak to $2\theta \sim 3.3°$ (corresponding to an interlayer spacing of *ca.* 27.6 Å) and the presence of at least two more (001) peaks. The expansion of interlayer spacing from 11.1 Å for the starting Na-RUB-18 to 27.6 Å occurs due to intercalation of cetytrimethylammonium (CTA) ions within the interlayer region of the layered silicate. The XRD patterns also indicate the formation of a mesostructured phase, with a basal peak at low 2θ values, which is ascribed to the (100) diffraction from a hexagonal arrangement of pores with d_{100} spacings (Table 1) of 45 Å (for samples prepared at Si/Al ratios = 5 and 10) and 45.7 Å (Si/Al ratio = 20). The as-synthesized materials also exhibit low intensity peaks in the 2θ region between 10 and 40°, which indicate that some of the crystallinity of the RUB-18 layered silicate is retained in the mesophases. The two step synthesis process of refluxing with the surfactant molecules and then hydrothermal treatment at 150 °C causes not only swelling of the Na-RUB-18 silicate but also intercalation of the surfactant molecules between the RUB-18 layers. The hydrothermal treatment transforms the expanded CTA intercalated RUB-18 layers into mesostructures.[25] Conversion to mesostructured materials may be aided by the increase in the flexibility of the layers due to some dissolution during the hydrothermal treatment step. It is also possible that some of the dissolved silica species can interact with dissolved Al species and surfactants to form a separate amorphous mesostructured phase.

The as-synthesized mesophases were subjected to template removal *via* a variety of methods. The XRD patterns of the resulting materials are shown in Fig. 1 and the d_{100} spacings are summarized in Table 1. The XRD pattern of the Si/Al = 5 sample, after surfactant removal *via* solvent extraction (Fig. 1A), generates a material (5 EXT) with a significant level of molecular ordering. A very weak basal (100) peak due to mesostructural ordering (d_{100} spacing = 43 Å) is observed, along with several sharp and relatively intense peaks in the 2θ region between 10 and 40° that are indicative of a significant level of molecular ordering in the solvent extracted 5 EXT sample. Sample 5 OXI also exhibits a broad low intensity basal (100) peak at a d_{100} spacing of 46.8 Å, and several broad and low intensity peaks in the 2θ region between 10 and 40°, indicating retention of some low level crystallinity. For both samples 5 EXT and 5 OXI, the peaks due to layered ordering of the expanded precursor silicate are not observed, which suggests that the lamellar ordering of RUB-18 does not survive the surfactant removal process. On the other hand, surfactant removal by calcination (sample 5 CAL) generates a mesoporous material that exhibits virtually no crystallinity, which is consistent with previous results.[24,26,27] Only the basal (100) peak from mesostructural ordering (with a d_{100} spacing of 45 Å) is observed; no peaks are observed in the 2θ region between 10 and 40°. Overall, the XRD patterns in Fig. 1A indicate that, at Si/Al ratio ~5, removal of the surfactant *via*

Table 1 Elemental composition and textural properties of the as-synthesized (AS) mesophases and surfactant-free aluminosilicate materials prepared at various Si/Al ratios following surfactant removal *via* calcination (CAL), extraction (EXT) and oxidation (OXI)

Sample	Si/Al ratio	d_{100} spacing (Å)	Surface area ($m^2\ g^{-1}$)	Pore volume ($cm^3\ g^{-1}$)	Pore size (Å)	Wall thickness[a] (Å)
5 AS	6.2	45.0				
5 CAL	6.2	45.0	347	0.44	24.0	28.0
5 OXI	6.6	46.8	283	0.37	25.6	28.4
5 EXT	8.0	43.1	388	0.46	23.5	26.6
10 AS	11.9	44.9				
10 CAL	11.9	42.3	334	0.32	23.0	25.8
10 OXI	11.0	44.0	238	0.25	24.0	26.8
10 EXT	14.8	40.0	374	0.29	23.8	22.4
20 AS	18.9	45.7				
20 CAL	18.9	41.5	267	0.20	22.5	25.4
20 OXI	17.4	43.1	141	0.15	23.6	26.2
20 EXT	23.9	41.5	197	0.16	22.5	25.4

[a] Wall thickness = a_o − pore size, where a_o = the lattice parameter obtained from the d_{100} spacing using the formula $a_o = 2d_{100}/\sqrt{3}$.

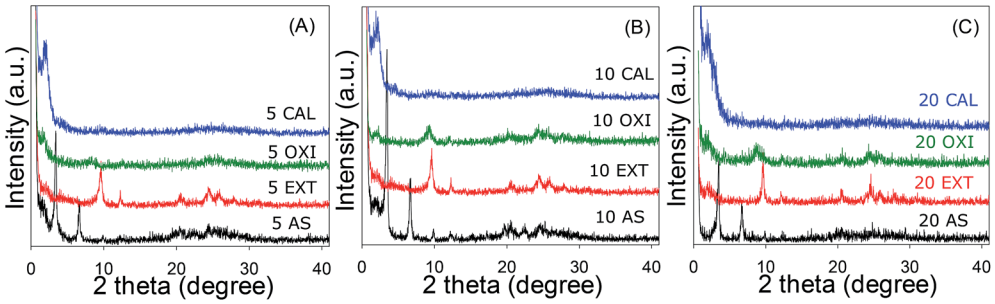

Fig. 1 Powder XRD patterns of aluminosilicate samples prepared at Si/Al ratios of: (A) 5; (B) 10; and (C) 20, before (AS) and after surfactant removal *via* extraction (EXT), oxidation (OXI) or calcination (CAL).

acid-mediated extraction is the best method for generating materials that exhibit both mesostructural characteristics and crystallinity. Some residual crystalline ordering is also retained in the oxidized sample, while direct calcination destroys the crystallinity.

The sample prepared at Si/Al ratio = 10, after surfactant removal by calcination (sample 10 CAL), exhibits no crystallinity (Fig. 1B); only the basal (100) peak from mesostructural ordering (d_{100} spacing = 42.3 Å) is observed with no peaks in the 2θ region between 10 and 40°. On the other hand, the H_2O_2-mediated oxidation sample (10 OXI) exhibits a broad low intensity basal (100) peak (d_{100} spacing = 44 Å) and several peaks in the 2θ region between 10 and 40° that are indicative of a significant level of molecular ordering. For the extracted sample (10 EXT), the basal (100) peak due to mesostructural ordering (d_{100} spacing = 40 Å) is observed along with several sharp and relatively intense peaks in the 2θ region between 10 and 40°. These latter peaks are indicative of a significant level of crystalline ordering in sample 10 EXT. A similar trend is observed for the sample prepared at Si/Al ratio = 20 (Fig. 1C); template removal *via* calcination (sample 20 CAL) generates a mesoporous material (with a d_{100} spacing of 41.5 Å) that exhibits no crystallinity, while the H_2O_2-mediated oxidation sample (20 OXI) exhibits a basal peak (d_{100} = 43.1 Å) and several peaks at 2θ = 10 to 40°, and surfactant removal *via* solvent extraction generates a material (sample 20 EXT) with a higher level of crystallinity and mesostructural ordering (d_{100} spacing = 41.5 Å).

IR spectroscopy was used to probe the retention of crystalline ordering in the as-synthesized mesophases and surfactant-free materials. The IR spectra of Na-RUB-18, the as-synthesized mesophases and surfactant-free materials are shown in Fig. 2. The spectrum of the parent Na-RUB-18 sample shows several bands in the region of framework vibration modes which indicate crystalline ordering, *i.e.*, bands at 825, 790 and 620 cm^{-1} are indicative of six or five membered ring subunits of T–O–T (T = Si or Al). The spectra of the as-synthesised (AS) mesophases exhibit these bands, which confirm that intercalation of CTA ions does not significantly affect crystallinity. The spectra of the 'oxidised' and 'extracted' samples exhibit the framework vibration modes. The resolution of the doublet at *ca.* 800 cm^{-1} is slightly reduced for the oxidised samples, while the resolution remains unchanged for the extracted samples. This suggests that crystallinity is retained to a greater extent for the extracted samples, which is consistent with the XRD patterns in Fig. 1. On the other hand, calcination results in a material that does not exhibit any framework bands; the doublet at 800 cm^{-1} and the peak at 600 cm^{-1} are not observed. This confirms that calcination destroys the crystalline ordering and generates an amorphous framework.

3.2 Efficiency of surfactant removal

Themogravimetric analysis (TGA) was used to probe the extent of surfactant removal from the as-synthesised mesophases. TGA curves for various as-synthesised mesophases before and after surfactant removal are shown in Fig. 3 (and the corresponding

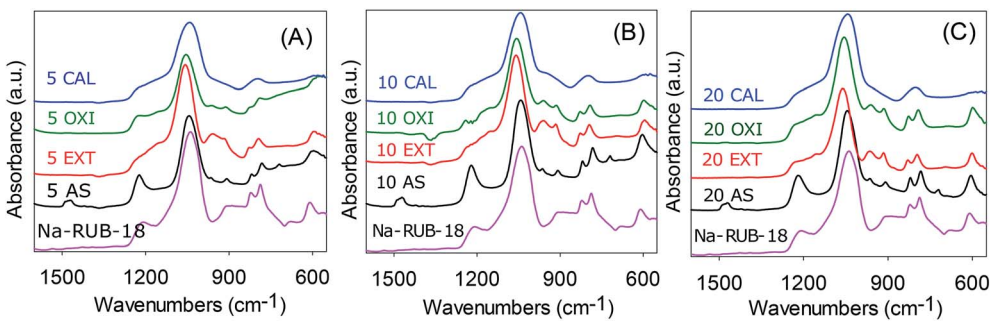

Fig. 2 Infrared spectra of Na-RUB-18 and aluminosilicate samples prepared at Si/Al ratios of; (A) 5; (B) 10; and (C) 20, before (AS) and after surfactant removal *via* extraction (EXT), oxidation (OXI) or calcination (CAL).

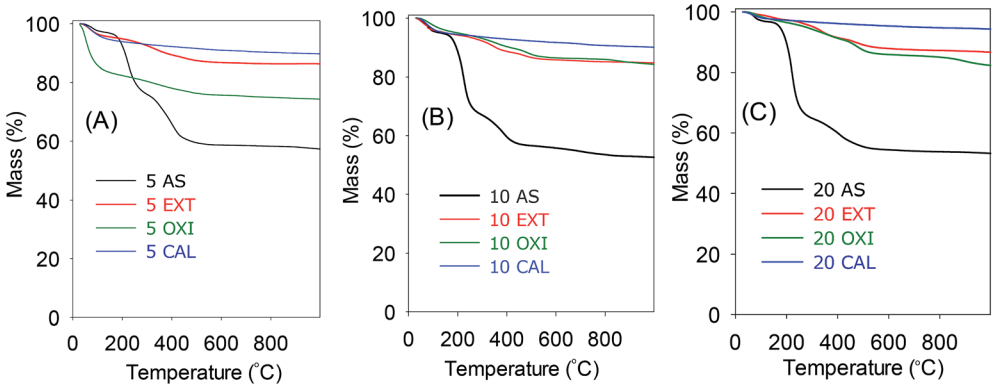

Fig. 3 Thermogravimetric analysis (TGA) curves of aluminosilicate samples prepared at Si/Al ratios of: (A) 5; (B) 10; and (C) 20, before (AS) and after surfactant removal *via* extraction (EXT), oxidation (OXI) or calcination (CAL).

differential thermogravimetric (DTG) profiles are shown in ESI Fig. S2†). The as-synthesised mesophases and all surfactant-free samples exhibit a mass loss below 150 °C due to desorption of physisorbed or residual solvents and/or water. For the as-synthesised (AS) mesophases, the mass loss corresponding to desorption of the cetyltrimethylammonium (CTA) ions occurs between 200 and 500 °C. The small mass loss (>4 wt%) of calcined (CAL) samples above 200 °C is due to dehydroxylation of the aluminosilica framework. The extracted and oxidised samples show mass losses of 5 and 10 wt%, respectively, between 200 and 400 °C. For the extracted samples, this mass loss is due to dehydroxylation of the aluminosilica framework, while for the oxidised samples, it is more likely that, in addition to dehydroxylation, removal of NH_3 groups also contributes to mass loss. Previous work has shown that the oxidation process (*i.e.*, treatment of organo-silicate phases with H_2O_2) does not oxidize/remove NH_3 groups.[32] Overall, the TGA curves and DTG profiles indicate that the oxidation and extraction processes are effective in removing the surfactant molecules. The absence of surfactant molecules in the calcined, oxidised and extracted samples is confirmed by the IR spectra (ESI Fig. S3†), wherein IR bands due to alkyl chain $(-CH_2-)_n$ vibrations (at 2700–3000 cm^{-1}) that are present for the as-synthesised mesophases are not observed in the calcined, oxidised and extracted samples.

3.3 Porosity

The nitrogen sorption isotherms of the surfactant-free materials are shown in Fig. 4 and the textural properties are summarized in Table 1. The pore size distribution curves are presented in Fig. 5. All the samples exhibit type IV isotherms, which are typical for mesoporous materials.[1–5] The isotherms show a mesopore filling step at P/P_o between 0.4 and 0.5, and a rise in adsorption at $P/P_o > 0.9$ due to interparticle voids.[33] Overall the isotherms of the calcined samples are typical for mesoporous materials, but differ from those of oxidized and extracted samples due to significant hysteresis at a relative pressure (P/P_o) of above 0.4, which may be caused by spaces between plate-like particles. Surfactant removal *via* solvent extraction (sample 5 EXT, Fig. 4A) generates a mesoporous material with a surface area of 388 $m^2\ g^{-1}$ and a pore volume of 0.46 $cm^3\ g^{-1}$, while the 'oxidised' sample (5 OXI) has a surface area of 283 $m^2\ g^{-1}$ and a pore volume of 0.37 $cm^3\ g^{-1}$. Calcination yields a material with a surface area of 347 $m^2\ g^{-1}$ and a pore volume of 0.44 $cm^3\ g^{-1}$. A similar trend in porosity is observed for samples prepared at a Si/Al ratio of 10, *i.e.*, extracted > calcined > oxidized. The surface area and pore volume of samples prepared at Si/Al ratios of 5 and 10 are comparable. For Si/Al ratio = 20 (Fig. 4C), all three samples have a surface area between 141 and 267 $m^2\ g^{-1}$ and the pore volume in the range of 0.15 to 0.20 $cm^3\ g^{-1}$. Thus a lower Al content generates samples with apparently lower porosity, which is consistent with the fact that the porosity of the present aluminosilicate materials is higher than that of analogous pure silica materials.[24]

The presence of well-ordered mesopores, of size 22.5–25.6 Å (Table 1), is illustrated by the pore size distribution curves in Fig. 5. The aluminosilicate materials have a relatively narrow pore size distribution in the lower mesopore range. This is a

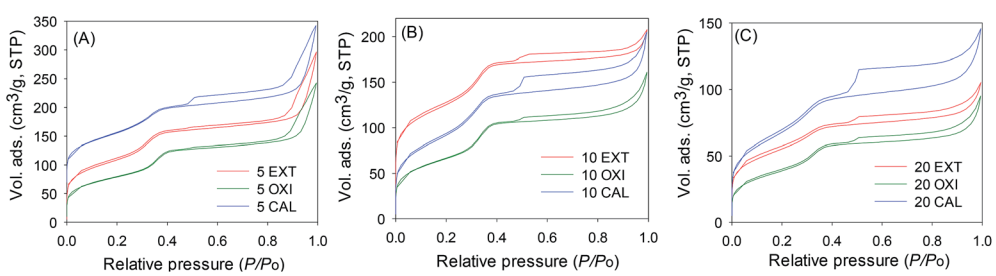

Fig. 4 Nitrogen sorption isotherms of aluminosilicate materials prepared at Si/Al ratios of: (A) 5; (B) 10; and (C) 20, after surfactant removal by calcination (CAL), extraction (EXT) or oxidation (OXI). Isotherms of 5 CAL and 10 EXT are offset (*y*-axis) by 60 and 40, respectively.

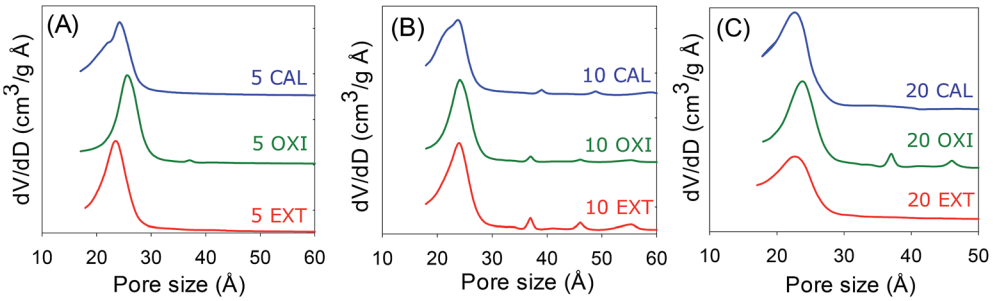

Fig. 5 Pore size distribution curves of aluminosilicate samples prepared at Si/Al ratios of; (A) 5; (B) 10; and (C) 20, after surfactant removal *via* calcination (CAL), oxidation (OXI) or extraction (EXT).

departure from mesoporous materials prepared using a similar route but with a conventional silica source wherein the pore size is much higher and typically above 40 Å.[1–5] In all three cases, the 'oxidised' samples have the marginally larger pore size. Furthermore, the pore size increases at higher Al content. The relatively small pore size of the materials means that they have relatively thick pore walls compared to conventional MCM-41 materials. The estimated wall thickness, which is summarized in Table 1, varies in the range of 22.4 to 28.4 Å and is typically above 25 Å. The pore wall thickness is lower than that of pure silica materials,[24] which is consistent with the higher porosity of the present aluminosilicate samples.

3.4 Electron microscopy

Electron microscopy shows that the Na-RUB-18 used in this study is a well ordered crystalline material (ESI Fig. S4†); the Na-RUB-18 material consists of thin tetragonal platelets and the SAED pattern corresponds to a highly crystalline material, which agrees well with the XRD pattern shown in ESI Fig. S1.† The SAED patterns (ESI Fig. S5†) suggest a lowering in crystallinity from the original RUB-18 to the as-synthesized aluminosilicate–surfactant mesophases and for both oxidized and extracted surfactant free samples. The SAED patterns also confirm a total loss of crystallinity for calcined samples. The SAED results, in agreement with powder XRD results, indicate that removal of the surfactant *via* extraction is the best method for generating materials retaining crystallinity, followed by oxidation, whereas calcination destroys the crystallinity. SEM images of the aluminosilicate–surfactant mesophases show that the platy morphology of the parent Na-RUB-18 silicate is maintained and that surfactant removal has no effect on the morphology (ESI Fig. S6–S8†). TEM images in Fig. 6 show that the crystal structure of the layers changes for samples prepared at Si/Al ratios of 5 and 10, and that a mesoporous structure is developed in the inner and outer areas of the plate-like particles of aluminosilicate–surfactant mesophases and surfactant free

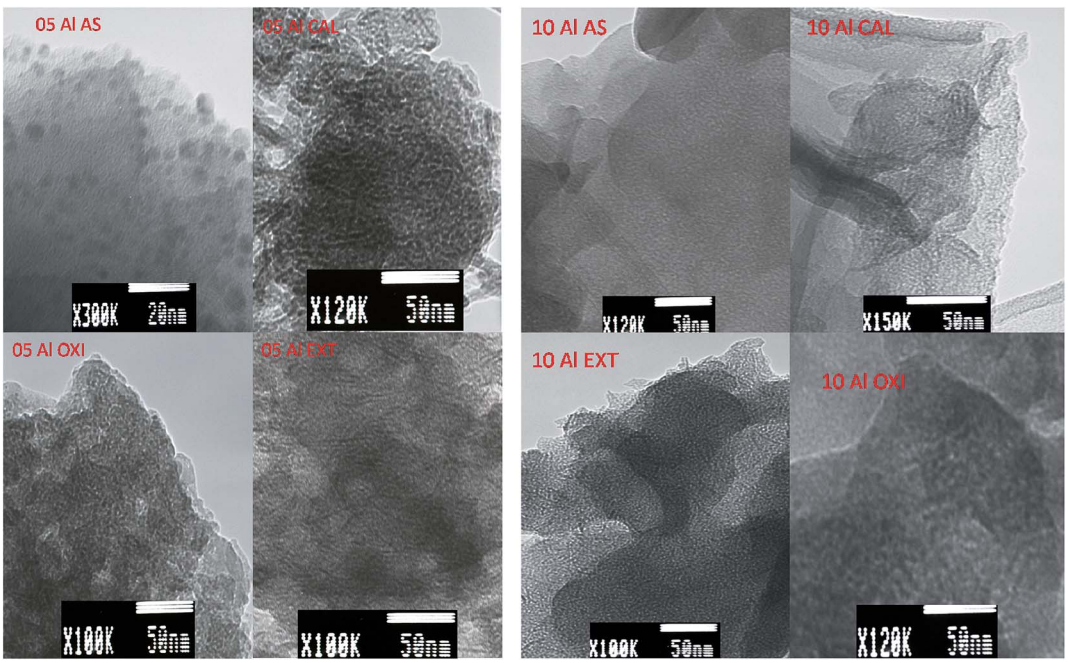

Fig. 6 TEM images of aluminosilicate samples prepared at Si/Al ratios of 5 or 10, before (AS) and after surfactant removal *via* calcination (CAL), oxidation (OXI) or extraction (EXT).

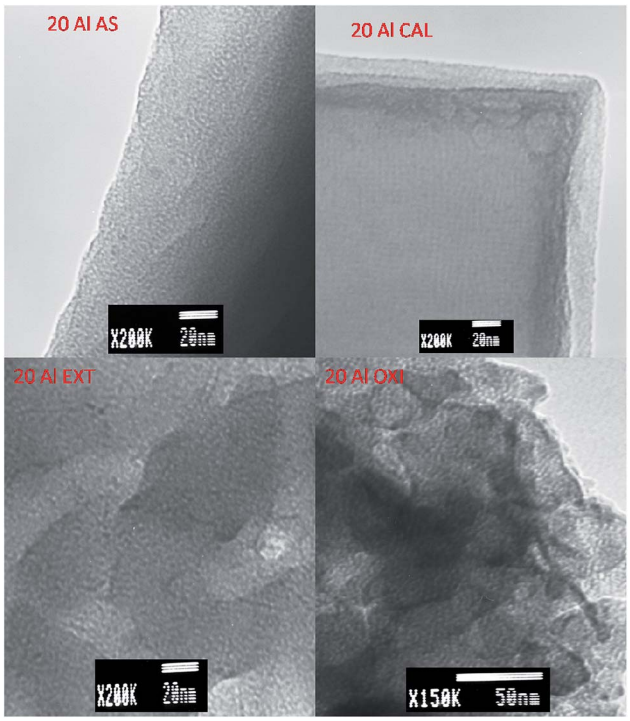

Fig. 7 TEM images of aluminosilicate samples prepared at a Si/Al ratio of 20, before (AS) and after surfactant removal *via* calcination (CAL), oxidation (OXI) or extraction (EXT).

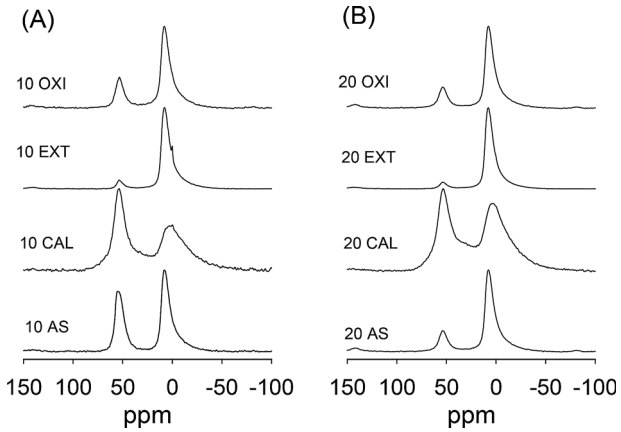

Fig. 8 ^{27}Al MAS NMR spectra of the as-synthesized (AS) and surfactant free aluminosilicate materials prepared at Si/Al ratios of 10 (A) and 20 (B) after surfactant removal *via* calcination (CAL), extraction (EXT) and oxidation (OXI).

aluminosilicate samples. For the sample prepared at a Si/Al ratio of 20, it is possible to observe in Fig. 7 a square-like structure, which seems to be an intermediate step of the solid-state transformation from the layered silicate Na-RUB-18 structure to the ordered mesoporous aluminosilicate materials.

3.5 Nature of Al and acidity/catalytic activity of mesoporous aluminosilicate materials

The Al content (Si/Al ratio) of the aluminosilicate materials is given in Table 1. As stated above, the Al content is close to the target Si/Al ratio in the synthesis gel mixture. Whilst surfactant removal by the oxidation route had little effect on the Al content (Table 1), extraction resulted in a decrease in Al content (*i.e.*, the Si/Al ratio increased from 6.2 to 8.0 for 5 EXT, 11.9 to 14.8 for 10 EXT and 18.9 to 23.9 for 20 EXT). This suggests that the solvent extraction process caused dealumination and preferential dissolution of alumina. We performed ^{27}Al MAS NMR spectroscopy in order to determine the nature of Al in the aluminosilicate samples and to monitor any changes in the Al environment after various surfactant removal routes. The ^{27}Al MAS NMR spectra of the samples, before and after surfactant removal, are shown in Fig. 8 for samples prepared at Si/Al ratios of 10 and 20. In both cases, the spectrum of the as-synthesised samples exhibits a resonance at *ca.* 54 ppm, which arises from tetrahedrally coordinated Al in an aluminosilicate framework, and also a peak at *ca.* 0 ppm from octahedrally coordinated extra-framework Al. The spectra indicate that the Al in the as-synthesised samples exists mainly in extra-framework positions especially for sample 20 AS. Sample 10 AS has much higher proportion of Al in framework sites. The proportion of Al in framework sites was noted to increase at higher Al content. In both cases the amount of framework Al increases on calcination so that most of the Al is in framework positions. This suggests that calcination inserts Al into framework positions. The spectra of the extracted and oxidized samples show a marked reduction in the proportion of framework Al. Surfactant removal *via* extraction and oxidation, therefore, causes dealumination.

The acidity of calcined samples was measured using thermally programmed desorption of cyclohexylamine. The method involves thermogravimetric analysis (TGA) of cyclohexylamine containing samples and determines the number of acid sites (principally proton sites) capable of interacting with the base after heat treatment at 80 °C and 250 °C.[29,30] The samples were exposed to liquid cyclohexylamine at room temperature after which they were kept overnight (at room temperature) and then in an oven at 80 °C for 2 h, so as to allow the base to permeate the samples. To probe the presence of strong acid sites, the base-containing samples were exposed to thermal treatment at 250 °C, which desorbed base molecules from weaker acid sites so as to determine the population of strong sites. The mass loss from desorption of the base from Brønsted acid sites (between 300 and 450 °C) was used to quantify the acid content (in mmol of cyclohexylamine per gram of samples) as shown in Table 2, assuming that each mole of cyclohexylamine corresponds to 1 mole of protons. The acidity values indicate that the incorporation of aluminum into the framework generates acid sites which are able to interact with the base. The total acidity is the highest for sample 5 CAL (0.68 mmol g^{-1}), decreases to 0.48 and 0.16 for samples 10 CAL and 20 CAL, respectively, in line with the Al content. The strong acid content of the directly calcined samples is either similar to (20 CAL) or slightly lower (5 CAL and 10 CAL) than the total acidity. This is a departure from what is observed for conventional mesoporous

Table 2 Elemental composition, acidity and catalytic activity of mesoporous aluminosilicate materials prepared at various Si/Al ratios following surfactant removal *via* direct calcination (CAL) or calcination after extraction (EXT + CAL) or oxidation (OXI + CAL)

Samples	Si/Al ratio	Acidity (mmol H^+ g^{-1})		Proportion of strong acidity (%)	Pentan-1-ol conversion (%)
		80 °C	250 °C		
5 CAL	6.2	0.68	0.56	82	91
5 OXI + CAL	6.6	0.38	0.37	97	77
5 EXT + CAL	8.0	0.33	0.35	100	75
10 CAL	11.9	0.48	0.40	83	78
10 OXI + CAL	11.0	0.50	0.47	94	83
10 EXT + CAL	14.8	0.31	0.31	100	71
20 CAL	18.9	0.16	0.18	100	58
20 OXI + CAL	17.4	0.23	0.25	100	65
20 EXT + CAL	23.9	0.18	0.16	89	55

aluminosilicates or Al-grafted aluminosilicate MCM-41 materials, where the proportion of strong acid sites is usually much lower (between 50 and 70%).[34] We attribute the strong acidity of the present aluminosilicate samples to the molecular ordering similar to that of zeolite materials.[35] It is noteworthy that the proportion of strong acid sites increases at lower Al content. The catalytic activity of the samples was tested using dehydration of pentan-1-ol at 200 °C.[36] As shown in Table 2, for the directly calcined samples, the conversion of pentan-1-ol is the highest for the most aluminous sample (5 CAL), reaching 91%, and reduces at lower Al content to 78% and 58% for samples 10 CAL and 20 CAL, respectively. Under similar conditions, proton exchanged forms of zeolite Y (Si/Al = 3.6) and conventional Al-MCM-41 materials (Si/Al = 20) achieved conversions of 88% and 39%, respectively. The catalytic data are consistent with the fact that the present aluminosilicate samples have a significant proportion of strong acid sites. The catalytic data also suggest that the present samples have a larger proportion of strong acid sites compared to conventional mesoporous aluminosilicates such as MCM-41.

Table 3 Textural properties of mesoporous aluminosilicate materials prepared *via* direct calcination (CAL) or calcination after extraction (EXT + CAL) or oxidation (OXI + CAL)

Sample	Surface area (m^2 g^{-1})	Pore volume (cm^3 g^{-1})
5 CAL	347	0.44
5 OXI	283	0.37
5 OXI + CAL	274	0.37
5 EXT	388	0.46
5 EXT + CAL	336	0.43
10 CAL	334	0.32
10 OXI	238	0.25
10 OXI + CAL	190	0.20
10 EXT	374	0.29
10 EXT + CAL	352	0.24
20 CAL	267	0.20
20 OXI	141	0.15
20 OXI + CAL	141	0.12
20 EXT	197	0.16
20 EXT + CAL	191	0.15

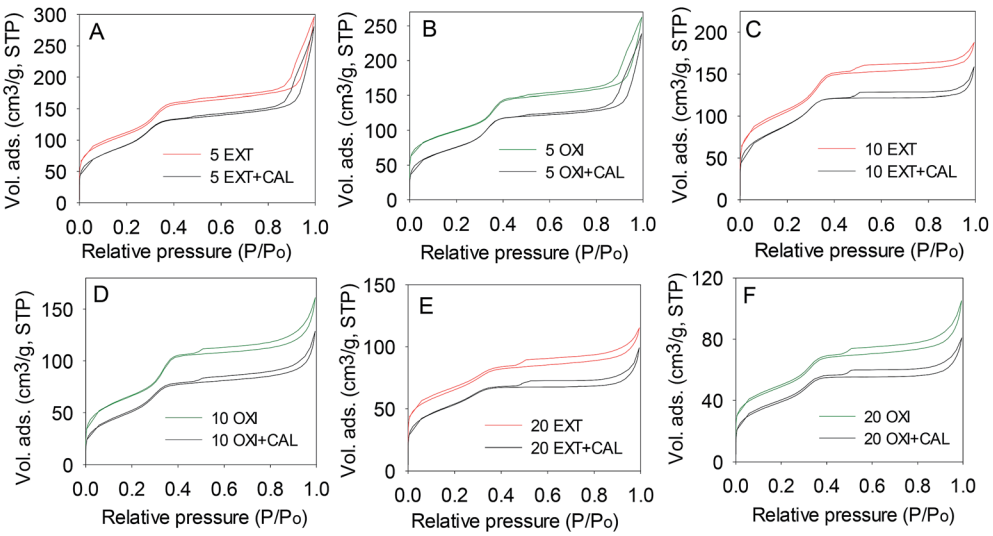

Fig. 9 Nitrogen sorption isotherms of extracted (A,C,E) or oxidized (B,D,F) aluminosilicate samples before and after calcination.

3.6 Thermal stability and acidity on calcination of extracted and oxidized samples

The thermal stability of extracted and oxidised samples was assessed by calcination. On calcination, the extracted and oxidised samples exhibit no basal (d_{100}) peak (ESI Fig. S9†) but nevertheless, nitrogen sorption isotherms (Fig. 9) show well defined mesopore filling steps for all the samples, which indicates that mesoporosity is retained after calcination. Interestingly, some high angle peaks are also observed in the XRD patterns of the OXI + CAL and EXT + CAL samples (ESI Fig. S9†), which suggests retention of some crystallinity. However, IR spectra (ESI Fig. S10†) show somewhat diminished framework bands after calcination; the doublet at 800 cm^{-1} and the peak at 600 cm^{-1} are observed but not well resolved. This indicates that calcination to some extent diminishes crystalline ordering. Overall, therefore, the mesoporosity of extracted and oxidised aluminosilicate samples was retained after calcination, but crystallinity was diminished but not completely destroyed as for directly calcined samples. The textural properties of the samples after calcination are summarized in Table 3; there are very little changes in the surface area and pore volume after the thermal treatment. The overall picture that emerges is that calcination after benign template removal is a viable route to prepare mesoporous aluminosilicates with some retained crystallinity from crystalline layered silicates.

Calcination of the EXT and OXI samples increases the proportion of framework Al as shown in Fig. 10. This indicates that calcination inserts Al into tetrahedral positions within the aluminosilicate framework. It is well known that Al can be inserted or re-inserted into tetrahedral positions of a silica/aluminosilica framework *via* anchoring onto silanol groups followed by calcination to form Si–O–Al bonds.[19–21] Such insertion of Al is the basis for the well-established Al-grafting or alumination processes.[19–21] In this work, the presence of non-framework Al (which is generated during template removal *via* oxidation or extraction – Fig. 8), and the fact that the mesophase will have a preponderance of silanol groups mean that during calcination of the EXT and OXI samples, the Al is re-inserted into the aluminosilicate framework with silanols acting as anchoring points. Such an insertion of Al should generate acid sites, as indeed shown in Table 2. In general the acidity generated is in line with the overall Al content (Table 2) of the samples and with the proportion of Al in tetrahedral positions (Fig. 10). The proportion of Al inserted into tetrahedral positions is greater at lower Al content as shown in Fig. 11; extracted and oxidized samples prepared at a Si/Al ratio of 5 have the lowest proportion of tetrahedral Al after calcination, while those prepared at a Si/Al ratio of 20 have the highest proportion. This explains why the trend in acidity for the samples is not directly related to the overall Al content (Table 2). In all cases the proportion of strong acid sites is typically above 90%. As shown in Table 2, the catalytic activity of the extracted or oxidized and then calcined samples is only slightly lower than that of the directly calcined samples. The slight decrease in catalytic activity is due to a lower acid content, which is a consequence of lower Al content (Tables 1 and 2). However, the decrease in activity is lower than the reduction in acidity, which suggests that per active site, the extracted or oxidized and then calcined samples are more active. Also, the oxidised and calcined (OXI + CAL) samples are in all cases more catalytically active than the equivalent extracted and calcined (EXT + CAL) samples. We attribute this to a higher content of tetrahedrally coordinated Al in the OXI + CAL samples as evidenced in Fig. 10 and 11.

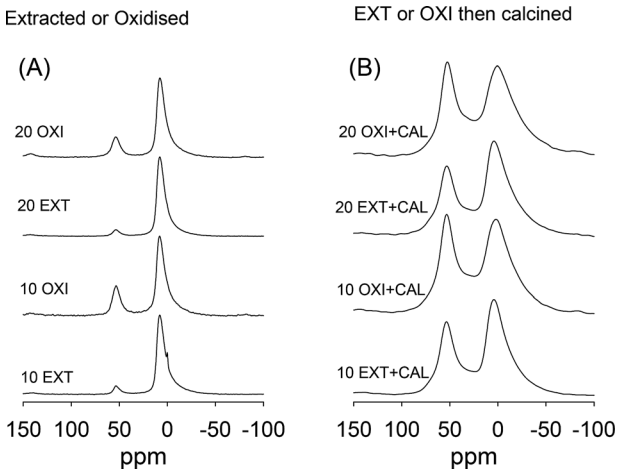

Fig. 10 ^{27}Al MAS NMR spectra of (A) extracted or oxidized surfactant free aluminosilicate materials prepared at Si/Al ratios of 10 or 20 and (B) after calcination.

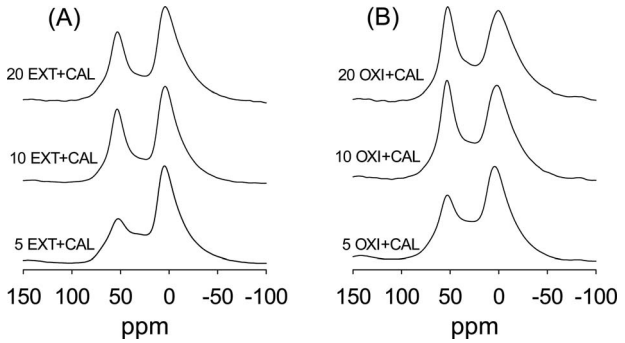

Fig. 11 ^{27}Al MAS NMR spectra of (A) extracted and then calcined, and (B) oxidized and then calcined mesoporous aluminosilicate materials.

4. Conclusions

Hydrothermal treatment, at 150 °C for 48 h, of the layered silicate, Na-RUB-18, in the presence of aluminum isopropoxide and cetyltrimethylammonium (CTA) ions generates molecularly ordered aluminosilicate–surfactant mesophases. Depending on the method (*i.e.* extraction, oxidation, and calcination) used to remove the surfactant, the transformation from mesophases to mesoporous materials takes place with retention of mesostructures with varying levels of crystallinity (for extracted and oxidized samples) or amorphous (for calcined samples) frameworks. The highest crystallinity in a surfactant-free mesostructure is achieved at a Si/Al ratio of 20 after surfactant removal *via*

solvent extraction in acidified ethanol. The textural properties of the mesoporous materials (surface area in the range of 141–388 $m^2 g^{-1}$ and pore volume in the range of 0.12–0.46 $cm^3 g^{-1}$) depend on the mode of surfactant removal and Si/Al ratio. The pore size of the materials (22–26 Å) is lower than that of conventional MCM-41 materials while the wall thickness (typically 25–28 Å) is much higher. The mesoporous aluminosilicates are strongly acidic with most of the acid sites generated (>80% and typically above 95%) classified as strong sites compared to between 50 and 70% for conventional direct mixed-gel synthesized or Al-grafted aluminosilicate MCM-41 materials. The mesoporous aluminosilicates exhibit attractive solid acid catalytic activity for the dehydration of pentan-1-ol, which is higher than that of conventional aluminosilicate MCM-41 materials. Overall, it is shown that the preparation of well-ordered surfactant-free aluminosilicate mesoporous materials with strong acidity is possible *via* the use of a crystalline layered silicate (Na-RUB-18) as the starting material.

Acknowledgements

We thank Dr David Apperley at the EPSRC Solid State NMR service (Durham) for the NMR spectra and are grateful to Prof Andrei Khlobystov for assistance with the TEM images.

References

1 (*a*) J. S. Beck, J. C. Vartuli, W. J. Roth, M. E. Leonowicz, C. T. Kresge, K. D. Schmitt, C. T.-W. Chu, D. H. Olson, E. W. Sheppard, S. B. McCullen, J. B. Higgins and J. L. Schlenker, *J. Am. Chem. Soc.*, 1992, **114**, 10834; (*b*) C. T. Kresge, M. E. Leonowicz, W. J. Roth, J. C. Vartuli and J. S. Beck, *Nature*, 1992, **359**, 710; (*c*) C. T. Kresge, M. E. Leonowicz, W. J. Roth and J. C. Vartuli, *US Pat.*, 5, 098, 684, 1992; (*d*) C. T. Kresge, M. E. Leonowicz, W. J. Roth and J. C. Vartuli, *US Pat.*, 5, 098, 684, 1992.

2 (*a*) A. Corma, *Chem. Rev.*, 1997, **97**, 2373; (*b*) M. E. Davis, *Nature*, 2002, **417**, 813; (*c*) J. Y. Ying, C. P. Mehnert and M. S. Wong, *Angew. Chem., Int. Ed.*, 1999, **38**, 56; (*d*) M. Linden, S. Schacht, F. Schuth, A. Steel and K. K. Unger, *J. Porous Mater.*, 1998, **5**, 177.

3 (*a*) A. Stein, *Adv. Mater.*, 2003, **15**, 763; (*b*) U. Ciesla and F. Schuth, *Microporous Mesoporous Mater.*, 1999, **27**, 131.

4 (*a*) A. Tagushi and F. Schuth, *Microporous Mesoporous Mater.*, 2004, **77**, 1; (*b*) G. Øye, J. Sjöblom and M. Stöcker, *Adv. Colloid Interface Sci.*, 2001, **89**, 439; (*c*) D. T. On, D. Desplantier-Giscard, C. Danumah and S. Kaliaguine, *Appl. Catal., A*, 2002, **222**, 299.

5 (*a*) J. S. Beck and J. C. Vartuli, *Curr. Opin. Solid State Mater. Sci.*, 1996, **1**, 76; (*b*) J. S. Beck, J. C. Vartuli, G. J. Kennedy, C. T. Kresge, W. J. Roth and S. E. Schramm, *Chem. Mater.*, 1994, **6**, 1816.

6 (*a*) J. M. Kim, S. K. Kim and R. Ryoo, *Chem. Commun.*, 1998, 259; (*b*) A. Sayari, *J. Am. Chem. Soc.*, 2000, **122**, 6504; (*c*) Y. Xia and R. Mokaya, *J. Mater. Chem.*, 2003, **13**, 657.

7 (*a*) P. T. Tanev, M. Chibwe and T. J. Pinnavaia, *Nature*, 1994, **368**, 321; (*b*) P. T. Tanev, Y. Liang and T. J. Pinnavaia, *J. Am. Chem. Soc.*, 1997, **119**, 8616; (*c*) S. A. Bagshaw, T. Kemmitt and N. B. Milestone, *Microporous Mesoporous Mater.*, 1998, **22**, 419; (*d*) W. Zhang, T. R. Pauly and T. J. Pinnavaia, *Chem. Mater.*, 1997, **9**, 2491; (*e*) T. R. Pauly, Y. Liu, T. J. Pinnavaia, S. J. L. Billinge and T. P. Rieker, *J. Am. Chem. Soc.*, 1999, **121**, 8835; (*f*) T. R. Pauly and T. J. Pinnavaia, *Chem. Mater.*, 2001, **13**, 987.

8 (*a*) S. S. Kim, W. Z. Zhang and T. J. Pinnavaia, *Science*, 1998, **282**, 1302; (*b*) S. S. Kim, Y. Liu and T. J. Pinnavaia, *Microporous Mesoporous Mater.*, 2001, **44**, 489.

9 (*a*) D. Zhao, J. Feng, Q. Huo, N. Melosh, G. H. Frederickson, B. F. Chmelka and G. D. Stucky, *Science*, 1998, **279**, 548; (*b*) D. Zhao, Q. Huo, J. Feng, B. F. Chmelka and G. D. Stucky, *J. Am. Chem. Soc.*, 1998, **120**, 6024; (*c*) D. Zhao, Q. Huo, J. Feng, J. Kim, Y. Han and G. D. Stucky, *Chem. Mater.*, 1999, **11**, 2668; (*d*) D. Zhao, J. Sun, Q. Li and G. D. Stucky, *Chem. Mater.*, 2000, **12**, 275.

10 (*a*) S. S. Kim, T. R. Pauly and T. J. Pinnavaia, *Chem. Commun.*, 2000, 1661; (*b*) P. Schmidt-Winkel, W. W. Lukens Jr, D. Zhao, P. Yang, B. F. Chmelka and G. D. Stucky, *J. Am. Chem. Soc.*, 1999, **121**, 254; (*c*) P. Schmidt-Winkel, W. W. Lukens Jr, P. Yang, D. I. Margolese, J. S. Lettow, J. Y. Ying and G. D. Stucky, *Chem. Mater.*, 2000, **12**, 686.

11 (*a*) Z. Yang, Y. Xia and R. Mokaya, *Adv. Mater.*, 2004, **16**, 727; (*b*) M. Kang, S. H. Yi, H. I. Lee, J. E. Yie and J. M. Kim, *Chem. Commun.*, 2002, 1944; (*c*) R. Ryoo, S. H. Joo and S. Jun, *J. Phys. Chem. B*, 1999, **103**, 7743.

12 (*a*) Y. Liu, W. Zhang and T. J. Pinnavaia, *J. Am. Chem. Soc.*, 2000, **122**, 8791; (*b*) Y. Liu, W. Zhang and T. J. Pinnavaia, *Angew. Chem., Int. Ed.*, 2001, **40**, 1255; (*c*) Z. Zhang, Y. Han, L. Zhu, R. Wang, Y. Yu, S. Qiu, D. Y. Zhao and F. S. Xiao, *Angew. Chem., Int. Ed.*, 2001, **40**, 1258; (*d*) Z. Zhang, Y. Han, F. S. Xiao, S. Qiu, L. Zhu, R. Wang, Y. Yu, B. Zou, Y. Wang, H. Sun, D. Y. Zhao and Y. Wei, *J. Am. Chem. Soc.*, 2001, **123**, 5014; (*e*) J. Liu, X. Zhang, Y. Han and F. S. Xiao, *Chem. Mater.*, 2002, **14**, 2536.

13 (*a*) K. R. Kloetstra, H. van Bekkum and J. C. Jansen, *Chem. Commun.*, 1997, 2281; (*b*) L. Huang, W. Guo, P. Deng, Z. Xue and Q. Li, *J. Phys. Chem. B*, 2000, **104**, 2817.

14 D. T. On and S. Kaliaguine, *Angew. Chem., Int. Ed.*, 2001, **40**, 3248.

15 D. T. On and S. Kaliaguine, *Angew. Chem., Int. Ed.*, 2002, **41**, 1036.

16 (*a*) W. P. Guo, L. M. Huang, P. Deng, Z. Y. Xue and Q. Z. Li, *Microporous Mesoporous Mater.*, 2001, **44**, 427; (*b*) W. P. Guo, C. R. Xiong, L. M. Huang and Q. Z. Li, *J. Mater. Chem.*, 2001, **11**, 1886; (*c*) P. H. R. P. Poladi and C. C. Landry, *J. Solid State Chem.*, 2002, **167**, 363.

17 (*a*) Y. Goto, Y. Fukushima, P. Ratu, Y. Imada, Y. Kubota, Y. Sugi, M. Ogura and M. Matsukata, *J. Porous Mater.*, 2002, **9**, 43; (*b*) Y. Xia and R. Mokaya, *J. Mater. Chem.*, 2004, **14**, 3427; (*c*) Y. Xia and R. Mokaya, *J. Mater. Chem.*, 2004, **14**, 863.

18 (*a*) A. Karlsson, M. Stocker and R. Schmidt, *Microporous Mesoporous Mater.*, 1999, **27**, 181; (*b*) F. S. Xiao, L. Wang, C. Yin, K. Lin, Y. Di, J. Li, R. Xu, D. S. Su, R. Schlogl, T. Yokoi and T. Tatsumi, *Angew. Chem., Int. Ed.*, 2006, **45**,

3090; (*c*) H. Wang and T. J. Pinnavaia, *Angew. Chem., Int. Ed.*, 2006, **45**, 7603.

19 (*a*) R. Mokaya and W. Jones, *Chem. Commun.*, 1997, 2185; (*b*) R. Ryoo, S. Jun, J. M. Kim and M. J. Kim, *Chem. Commun.*, 1997, 2225; (*c*) R. Mokaya and W. Jones, *Chem. Commun.*, 1998, 1839; (*d*) Z. H. Luan, M. Hartmann, D. Y. Zhao, W. Z. Zhou and L. Kevan, *Chem. Mater.*, 1999, **11**, 1621; (*e*) R. Mokaya and W. Jones, *J. Mater. Chem.*, 1999, **9**, 555.

20 (*a*) R. Mokaya, *Angew. Chem., Int. Ed.*, 1999, **38**, 2930; (*b*) R. Mokaya, *Chem. Commun.*, 2001, 633; (*c*) R. Mokaya, *ChemPhysChem*, 2002, 360; (*d*) A. S. O'Neil, R. Mokaya and M. Poliakoff, *J. Am. Chem. Soc.*, 2002, **124**, 10636; (*e*) Y. Xia and R. Mokaya, *Microporous Mesoporous Mater.*, 2004, **74**, 179.

21 (*a*) R. Mokaya, *Chem. Commun.*, 2000, 1891; (*b*) R. Mokaya, *J. Catal.*, 1999, **186**, 470; (*c*) R. Mokaya, *J. Catal.*, 2000, **193**, 103; (*d*) R. Mokaya, *Adv. Mater.*, 2000, **12**, 1681; (*e*) R. Mokaya, *Chem. Commun.*, 2000, 1541; (*f*) J. T. Tompkins and R. Mokaya, *ACS Appl. Mater. Interfaces*, 2014, **6**, 1902.

22 (*a*) M. Choi, H. E. Cho, R. Srivastava, C. Venkatesan, D. H. Choi and R. Ryoo, *Nat. Mater.*, 2006, **5**, 718; (*b*) R. Srivastava, M. Choi and R. Ryoo, *Chem. Commun.*, 2006, 4489; (*c*) K. Kim, M. Choi and R. Ryoo, *J. Catal.*, 2010, **269**, 219.

23 (*a*) S. C. Christiansen, D. Y. Zhao, M. T. Janicke, C. C. Landry, G. D. Stucky and B. F. Chmelka, *J. Am. Chem. Soc.*, 2001, **123**, 4519; (*b*) R. Mokaya, *Chem. Commun.*, 2001, 1092; (*c*) Y. Xia, J. J. Titman and R. Mokaya, *J. Phys. Chem. B*, 2004, **108**, 11361; (*d*) Y. Xia and R. Mokaya, *Microporous Mesoporous Mater.*, 2006, **94**, 295; (*e*) Y. Xia and R. Mokaya, *J. Phys. Chem. B*, 2006, **110**, 9122; (*f*) L. Q. Wang and G. J. Exarhos, *J.Phys. Chem. B*, 2003, **107**, 443.

24 N. Alam and R. Mokaya, *J. Mater. Chem.*, 2008, **18**, 1383.

25 (*a*) T. Yanagisawa, T. Shimizu, K. Kuroda and C. Kato, *Bull. Chem. Soc. Jpn.*, 1990, **63**, 988; (*b*) S. Inagaki, Y. Fukushima and K. Kuroda, *J. Chem. Soc., Chem. Commun.*, 1993, 680.

26 H. F. Greer, W. Zhou, N. Alam and R. Mokaya, *J. Mater. Chem.*, 2012, **22**, 23141.

27 R. Garcıa, I. Dıaz, C. Marquez-Alvarez and J. Perez-Pariente, *Chem. Mater.*, 2006, **18**, 2283.

28 M. Borowski, I. Wolf and H. Gies, *Chem. Mater.*, 2002, **14**, 38.

29 (*a*) J. A. Ballantine, J. H. Purnell and J. M. Thomas, *Clay Miner.*, 1983, **18**, 347; (*b*) C. Breen, *Clay Miner.*, 1991, **26**, 487.

30 (*a*) R. Mokaya and W. Jones, *J. Catal.*, 1997, **172**, 211; (*b*) R. Mokaya and W. Jones, *Chem. Commun.*, 1996, 983; (*c*) R. Mokaya, W. Jones, S. Moreno and G. Poncelet, *Catal. Lett.*, 1997, **49**, 87; (*d*) M. Pichowicz and R. Mokaya, *Chem. Commun.*, 2001, 2100.

31 S. Vortmann, J. Rius, S. Siegmann and H. Gies, *J. Phys. Chem. B*, 1997, **101**, 1292.

32 I. Melian-Cabrera, F. Kapteijn and J. A. Moulijn, *Chem. Commun.*, 2005, 2744.

33 J. Rathousky, A. Zukal, O. Franke and G. Shulzekloff, *J. Chem. Soc., Faraday Trans.*, 1994, **90**, 2821.

34 (*a*) R. Mokaya and W. Jones, *Phys. Chem. Chem. Phys.*, 1999, **1**, 207; (*b*) R. Mokaya, *J. Phys. Chem. B*, 2000, **104**, 8279; (*c*) R. Mokaya, *J. Phys. Chem. B*, 2003, **107**, 6954.

35 E. Masika and R. Mokaya, *Chem. Mater.*, 2011, **23**, 2491.

36 (*a*) R. Mokaya and W. Jones, *J. Chem. Soc., Chem. Commun.*, 1994, 929; (*b*) J. Bovey and W. Jones, *J. Mater. Chem.*, 1995, **5**, 2027; (*c*) F. Kooli, J. Bovey and W. Jones, *J. Mater. Chem.*, 1997, **7**, 153.